Indian J Phys (July 2023) 97(8):2355–2362
https://doi.org/10.1007/s12648-022-02547-1

ORIGINAL PAPER

First-principles study of properties of $X_3Sb_2Au_3$ (X = K, Rb) ternary compounds for photovoltaic applications

M Mbilo[1]*, R Musembi[1] and D P Rai[2]

[1]Department of Physics, University of Nairobi, Nairobi, Kenya

[2]Department of Physics, Physical Sciences Research Center (PSRC), Pachhunga University College, Mizoram University, Aizawl, India

Received: 07 June 2022 / Accepted: 27 November 2022 / Published online: 14 December 2022

Abstract: In this work, the structural, electronic, elastic, and optical properties of $X_3Sb_2Au_3$ (X = K, Rb) ternary compounds have been investigated using the density-functional theory method as implemented in the quantum espresso package. The generalized gradient approximation has been adopted in performing the calculations. The computed lattice parameters have been found to be in agreement with the available experimental and theoretical results. The $K_3Sb_2Au_3$ and $Rb_3Sb_2Au_3$ compounds have been found to be semiconductors with direct bandgaps of 1.236 eV and 1.353 eV, respectively. The compounds have also been found to be mechanically stable at zero pressure, ductile, and nearly metallic and therefore possess suitable attributes for industrial applications. The complex dielectric functions, absorption coefficients, reflectivity, refractive index, and energy loss spectra have also been presented. Refractive indices of 3.41 and 3.11 for $K_3Sb_2Au_3$ and $Rb_3Sb_2Au_3$ have also been calculated. The high refractive indices, high absorption coefficients, as well as the wide energy coverage of the absorption spectra, mostly in the ultraviolet–visible (UV–Vis) regions make the $K_3Sb_2Au_3$ and $Rb_3Sb_2Au_3$ compounds excellent UV–Vis light absorbers which are some of the essential characteristics for materials for photovoltaic applications.

Keywords: DFT; Bandgaps; Ternary compounds; Optical properties; Photovoltaic applications

1. Introduction

Ever since the 1970's global energy crisis, the gap between the energy demand and supply chain has persisted to widen. Due to the global transition to industrialization and urbanization, the need for renewable and clean solar energy has been on the rise [1]. In photovoltaic fabrication, one of the most important components is the light absorbing layer also known as the active layer. The solar cells' active layer may be derived from either organic, inorganic, or organic–inorganic blended materials with a suitable bandgap for photon absorption [2]. Among the materials used as absorbers, ternary compounds have been extensively investigated owing to their potential applications in the field of photovoltaics [3, 4]. The ternary compounds with the ABC_2- type crystal structure are grouped into chalcogenides ($A^IB^{III}C_2^{VI}$) and pnictides ($A^{II}B^{IV}C_2^{V}$) [5]. These materials have narrow bandgaps in the range of the solar spectrum thus they are appropriate for solar cell applications [5].

Irfan et al. [6] studied the structural, electronic, thermophysical, and optical properties of $K_3Cu_3P_2$ and $K_3Ni_2P_2$ pnictide materials by employing DFT for potential application in thermophysical and optoelectronic fields. Li et al. [7] investigated the thermoelectric properties as well as electronic structures of ABX_2 materials by using first-principles calculation and reported their prospective applications in thermoelectric devices. Iqbal et al. [8] carried out a first-principles study on the electronic and optical properties of $AlGaAs_2$ and $AlGaSb_2$ compounds for possible applications in thermoelectric and optoelectronic. A similar study was carried out on $CdSiAs_2$ chalcopyrite [9]. Mechanical properties of $BeSiP_2$ and $BeGeP_2$ chalcopyrites have also been investigated [5]. In a different study by Fai et al., DFT + U approach was employed to study the vibrational, thermoelectric, and electronic properties of $AgInTe_2$ and $AgGaTe_2$ chalcopyrite [10]. Recently, the physical properties of $SrPd_2Sb_2$ chalcopyrite have been studied using the DFT approach [11]. Further

*Corresponding author, E-mail: mwendebilo@students.uonbi.ac.ke

DFT studies on the properties of ABC_2- type ternary compounds have been reported in several treatise [12–19]. Indeed, employing the computational-based tools could help in gaining insightful information for proposing photo-related applications of the investigated structures [20–22]. In fact, in the field of photovoltaic solar cells, the solid-state type of absorber has been dominant ever since first device was unveiled by Chapin et al. [23] in 1954. Recently, computational designs using the density-functional theory have played an important role in the development of the metal halide perovskite from its debut in 2012 to its current high conversion efficiency of 25% in the shortest period in history of photovoltaics [24]. The use of insilico techniques may enable further advancement toward the Shockley–Queisser limit [25, 26] through bandgap engineering, as well as search for new compounds via combination of different elements.

Despite many first-principles investigations existing in the literature on ABC_2- type ternary semiconductor compounds, the full potential for applications of these materials has not yet been realized. Therefore, there is a need to do more investigations on the properties of these materials for the full realization of their applications. In this study, we have employed a density-functional theory to analyze the properties of $X_3Sb_2Au_3$ (X = K, Rb) ternary compounds. The properties that have been emphasized on are the structural, electronic, elastic, and optical properties in order to get insights into their optoelectronic potential. The motivation for this investigation came from the fact that there are few theoretical and experimental studies reported in the literature [27, 28] on the crystal structure of $K_3Sb_2Au_3$ and $Rb_3Sb_2Au_3$ ternary compounds. Furthermore, apart from the proposed crystal structure, studies on their properties had not been done previously.

2. Computational methods

In this investigation, a plane wave pseudopotential method within the Kohn–Sham framework DFT as implemented in the QE package [29] was used to perform the theoretical calculations [30, 31]. Generalized gradient approximation with Perdew–Burke–Ernzerhof (PBE) [32] functional was used. The $K_3Sb_2Au_3$ and $Rb_3Sb_2Au_3$ crystal structure input files were obtained from the materials project database [28] and the materials cloud input generator implemented in quantum espresso was used to generate the PWscf input file as well as the pseudopotentials [33] for DFT calculations. The lattice parameters of the $K_3Sb_2Au_3$ crystal used were $a = b = c = 15.3919$ a.u and $\alpha = \beta = \gamma = 45.985°$, while the lattice parameters of the $Rb_3Sb_2Au_3$ crystal were $a = b = c = 15.665$ a.u and $\alpha = \beta = \gamma = 47.353°$. These lattice parameters are of the rhombohedral crystal structure representation. The cutoff energy of 160 Ry and Monkhorst–Pack k-point mesh of $8 \times 8 \times 8$ with offset of 1 were used in this work. These values were arrived at by minimizing the total energy with respect to the cutoff energy and k-points. Geometry optimization was performed by minimizing the total energy with respect to the lattice constants. The optimized lattice constants, cutoff energy and k-points thus obtained were used in doing further calculations of electronic, elastic, mechanical, and optical properties.

3. Results and discussion

3.1. Structural properties

Both the $K_3Sb_2Au_3$ and $Rb_3Sb_2Au_3$ compounds crystallize in the trigonal crystal symmetry belonging to the space group orientation R3m (space number 166) [28]. The total energies of the crystal structures were calculated at different values of the lattice constants in the rhombohedral representation as shown in Fig. 1.

The computed total energy and lattice constant values were fitted in the Birch–Murnaghan equation of state [34] to obtain the ground state structural properties as shown in Table 1. The ground state lattice parameters obtained for the $K_3Sb_2Au_3$ and $Rb_3Sb_2Au_3$ are consistent with the ones reported in other works [27, 28].

The crystal structures of $K_3Sb_2Au_3$ and $Rb_3Sb_2Au_3$ compounds are presented in Fig. 2 below.

The bond lengths and bond angles of the $K_3Sb_2Au_3$ and $Rb_3Sb_2Au_3$ crystal structures were obtained as shown in Table 2.

The calculated bond lengths shown in Table 2 corroborates similar values to the ones reported in the literature for the crystal structures of $K_3Sb_2Au_3$ and $Rb_3Sb_2Au_3$ [27, 28] as previously proposed.

3.2. Electronic properties

The optimized $K_3Sb_2Au_3$ and $Rb_3Sb_2Au_3$ structures were used in the calculation of electronic properties. The band structure and the projected density of states (PDOS) of the $K_3Sb_2Au_3$ and $Rb_3Sb_2Au_3$ compounds are presented in Figs. 3 and 4 below.

From the band structure plots of the two compounds, (see Figs. 3(a) and 4(a)); it can be observed that the $K_3Sb_2Au_3$ and $Rb_3Sb_2Au_3$ ternary compounds are semiconductors with bandgaps of 1.236 eV and 1.353 eV, respectively. The calculated bandgaps lie within the range of 1–3.5 eV for ternary compounds covering the electromagnetic spectrum in the visible region [5, 35]. The computed bandgaps are slightly below the values reported

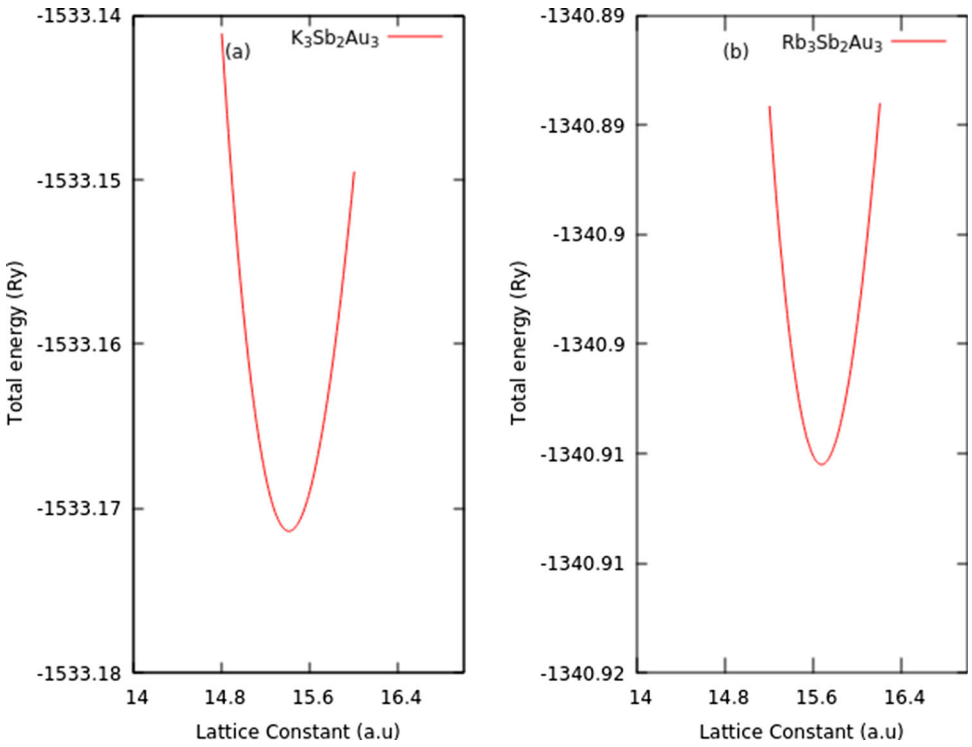

Fig. 1 Schematic showing the convergence of the total energy with the lattice constants of (**a**) $K_3Sb_2Au_3$ and (**b**) $Rb_3Sb_2Au_3$ ternary compounds

Table 1 Ground state lattice and structural Properties of the rhombohedral lattice of the $K_3Sb_2Au_3$ and $Rb_3Sb_2Au_3$ ternary compounds obtained by fitting the total energy and lattice constant values in the Birch–Murnaghan equation of state

Structural properties	$K_3Sb_2Au_3$		$Rb_3Sb_2Au_3$	
Lattice parameter a_o (a.u)	This work	Other work	This work	Other work
	15.3977	15.3919	15.6671	15.665
Bulk modulus B_o (GPa)	16.4		15.3	
Ist pressure derivative B_o^I	0.503		0.507	
Ground state energy E_o (Ry)	− 1533.17368		− 1340.91232	
Equilibrium volume V_o (Bohrs.)^3	3650.60		3845.62	

elsewhere [28], this may be attributed to the known fact that GGA-PBE tends to underestimate bandgap. The valence band maxima and the conduction band minima of both materials are at the same symmetry points in the first Brillouin zone which implies the direct nature of the bandgaps. The Fermi level lies between the valence band maxima and conduction band minima and it governs the possibility of electrons occupying different energy levels. The magnitude of the Fermi level predicts the rate of electronic transitions. The nearer the Fermi level is to the conduction band, the lesser the energy required for the electrons to transition from the valence to the conduction bands. In the considered − 6 to 6 eV energy region, the valence bands were majorly formed by the Au-4*d* state in the region − 6 to − 3.5 eV with little contribution by the other states. The valence band in the energy regions − 3 eV to the Fermi level is mainly formed by Sb-3*p* with a small contribution from the other states. The conduction band was formed mainly by Sb-3*p* states with low contribution from the other states. From the band structure and projected density of states plots, it is noticed that there are dense and close-packed energy bands that are intermediate in the energy region − 6 eV to − 4 eV of the valence band implying interband transitions, thus suggesting the materials may find applications in solar cells [6].

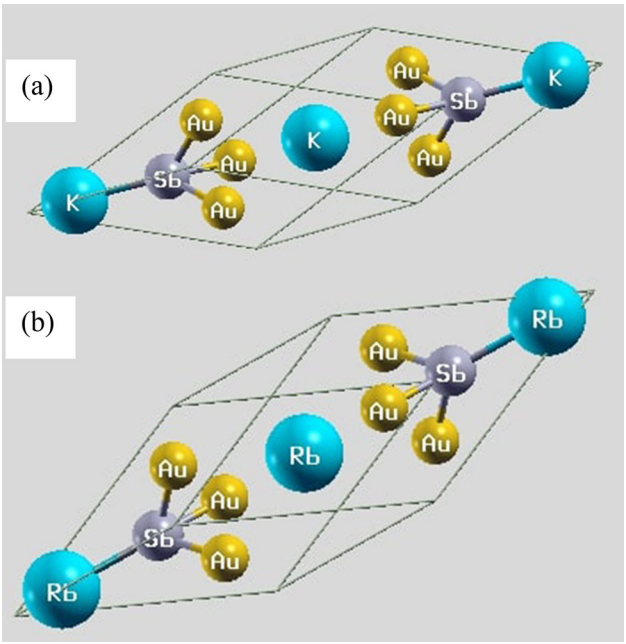

Fig. 2 Rhombohedral representation of the crystal structures of (**a**) $K_3Sb_2Au_3$ and (**b**) $Rb_3Sb_2Au_3$ ternary compounds

Table 2 The bond lengths and bond angles as calculated for the $K_3Sb_2Au_3$ and $Rb_3Sb_2Au_3$ crystal structures

Material bonding	Lattice values
$K_3Sb_2Au_3$	
Bond lengths (a.u)	
K–Sb	6.6490
Au–Sb	5.1127
Bond angles (Degrees)	
K–Sb–Au	137.240
K–Au–Sb	24.307
Au–K–Sb	18.453
$Rb_3Sb_2Au_3$	
Bond lengths (Bohr)	
Rb–Sb	6.9102
Au–Sb	5.0888
Bond angles (Degrees)	
Rb–Sb–Au	134.460
Rb–Au–Sb	26.416
Au–Rb–Sb	19.124

3.3. Elastic properties

Both $K_3Sb_2Au_3$ and $Rb_3Sb_2Au_3$ crystal structures belong to the rhombohedral (I) class representation which features six independent elastic constants C_{11}, C_{12}, C_{13}, C_{14}, C_{33}, and C_{44} [36]. The four necessary and sufficient conditions for elastic stability of the rhombohedral (I) class representation [36] include;

$$\begin{cases} C_{11} > |C_{12}|;\ C_{44} > 0, \\ C_{13}^2 < \frac{1}{2}C_{33}(C_{11} + C_{12}) \\ C_{14}^2 < \frac{1}{2}C_{44}(C_{11} - C_{12}) = C_{44}C_{66} \end{cases} \quad (1)$$

The conditions in Eq. (1) are satisfied using the independent elastic constants in Table 3. This implies that both $K_3Sb_2Au_3$ and $Rb_3Sb_2Au_3$ are mechanically stable. From these elastic constants, other mechanical properties are extracted and shown in Table 4.

The ductile (ionic) and brittle (covalent) nature of materials is determined by Pugh's ratio B/G and Poisson's ratio, n [37]. A material is said to be ductile if B/G > 1.75 whereas materials are said to be brittle if B/G < 1.75. Thus, in our study, both $K_3Sb_2Au_3$ and $Rb_3Sb_2Au_3$ are ductile. The Poisson's ratio n = 0.1, 0.25, and 0.33 for pure covalent, ionic, and metallic bonds, respectively [38]. Therefore, we can conclude that the materials studied are strongly dominated by the metallic character. The stiffness of a material is measured by Young's modulus [39]. A high value for Young's modulus implies more stiffness while a low value for Young's modulus implies less stiffness [39]. Debye temperature is a measure linked to a material's physical properties [40]. It is obtained from the elastic constants [41] as well as the average Debye sound velocities according to the relation [42]:

$$\theta_D = \frac{h}{K_B}\left(\frac{3}{4\pi V_a}\right)^{\frac{1}{3}} V_m \quad (2)$$

where V_a is the volume of a unit cell while h and K_B refer to the Planck's and Boltzmann's constants, respectively [42].

3.4. Optical properties

To explore the material's prospects for optoelectronic applications, it is important to investigate its optical properties. The optical properties describe the electromagnetic frequency response of solid-state materials to the incident photon energies [43]. In this work, the frequency-dependent dielectric constants were computed using the Sternheimer equation by neglecting the local fields without summing up the empty bands [44] in the rhombohedral representation. The complex dielectric wave function which describes the electron response in a material is given as [45];

$$\varepsilon(\omega) = \varepsilon_1(\omega) + i\varepsilon_2(\omega) \quad (3)$$

where $\varepsilon_1(\omega)$ refers to the real part and $\varepsilon_2(\omega)$ imaginary part of the dielectric wave function. From the computed $\varepsilon_1(\omega)$ and $\varepsilon_2(\omega)$ values, the other optical constants including the refractive index $n(\omega)$, absorption coefficients $\alpha(\omega)$, energy

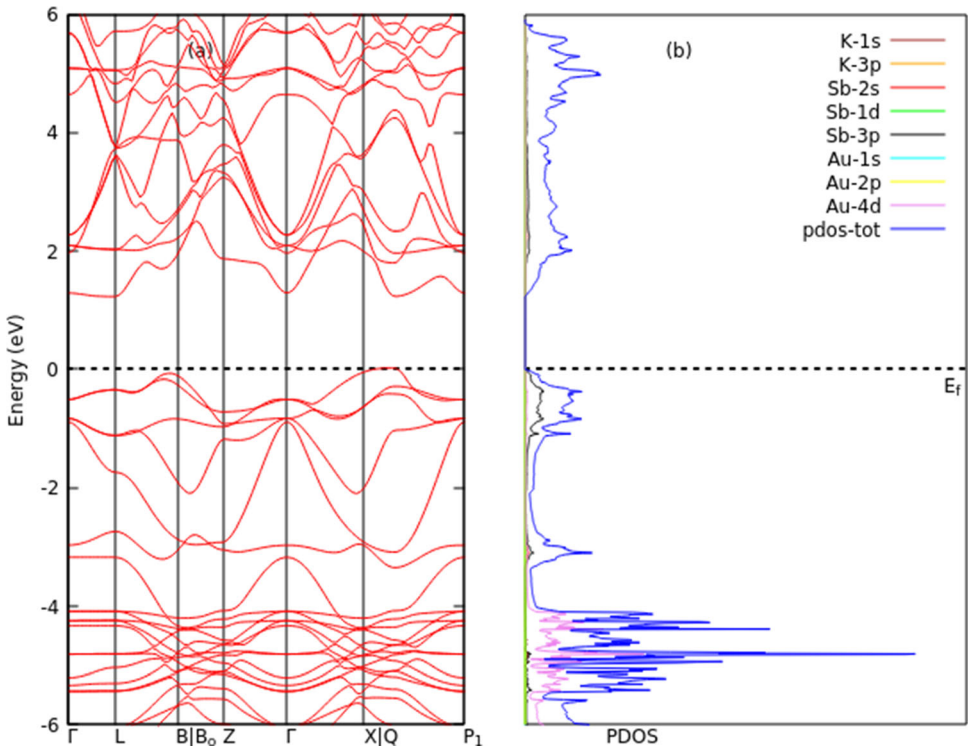

Fig. 3 The calculated electronic properties (**a**) Band structure and (**b**) PDOS of $K_3Sb_2Au_3$ ternary compound

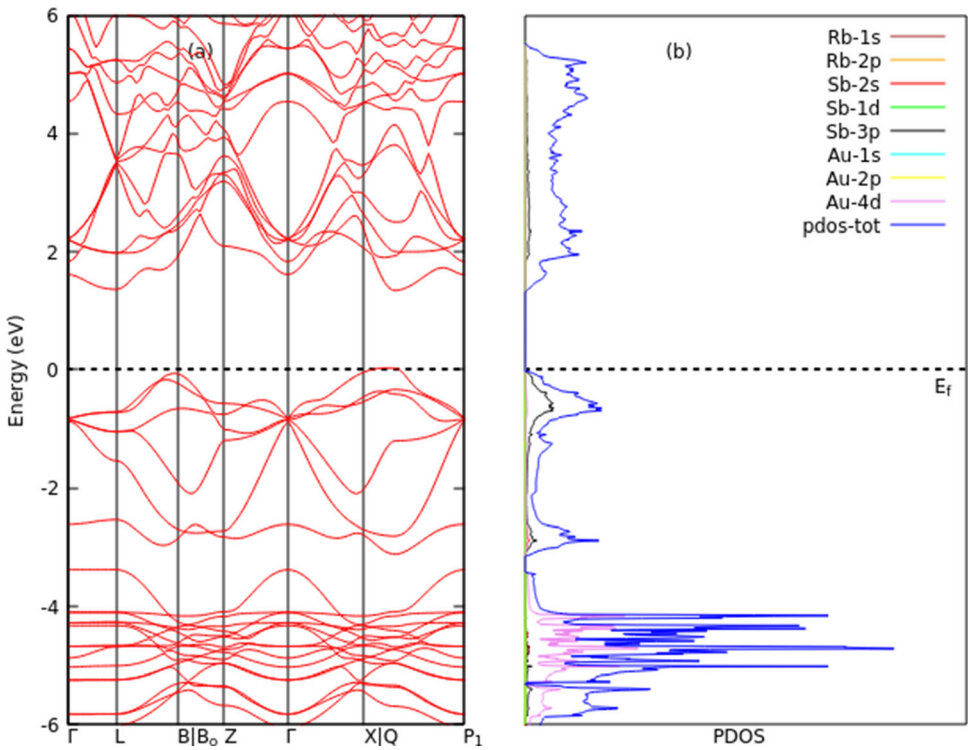

Fig. 4 The calculated electronic properties (**a**) Band structure and (**b**) PDOS of $Rb_3Sb_2Au_3$ ternary compound

loss spectrum $L(\omega)$, and reflectivity $R(\omega)$ were calculated using the equations [17, 46, 47].

A description of optical absorption is represented by the imaginary parts of the dielectric function. The absorption onsets in the $\varepsilon_2(\omega)$ curve was found to be 1.23 eV and 1.34 eV for $K_3Sb_2Au_3$ and $Rb_3Sb_2Au_3$, respectively [see Fig. 5(a)]. These values are consistent with the ones obtained from the band structure. The refractive index of materials is related to the real part of the dielectric function according to the relation $= \sqrt{\varepsilon_1(0)}$. Starting from the zero-

Table 3 Computed elastic Constants C_{ij} (GPa) of $K_3Sb_2Au_3$ and $Rb_3Sb_2Au_3$ ternary compounds

Compound	C_{11}	C_{12}	C_{13}	C_{14}	C_{33}	C_{44}
$K_3Sb_2Au_3$	25.0	8.2	13.9	5.5	38.8	7.4
$Rb_3Sb_2Au_3$	22.7	6.7	11.3	5.4	36.5	6.5

Table 4 Voigt-Reuss-Hill Approximations of bulk modulus *B* (GPa), Young's modulus *E* (GPa), Shear modulus *G* (GPa), Pugh's ratio B/G, Poisson's ratio *n*, average Debye sound velocities V_m (m/s) and Debye temperatures θ_D (K) of $K_3Sb_2Au_3$ and $Rb_3Sb_2Au_3$ ternary compounds

Compound	*B*	*E*	*G*	*B/G*	*n*	V_m	θ_D
$K_3Sb_2Au_3$	17	16	6	2.73	0.32	1067.73	100.27
$Rb_3Sb_2Au_3$	14	14	5	2.66	0.31	975.99	88.63

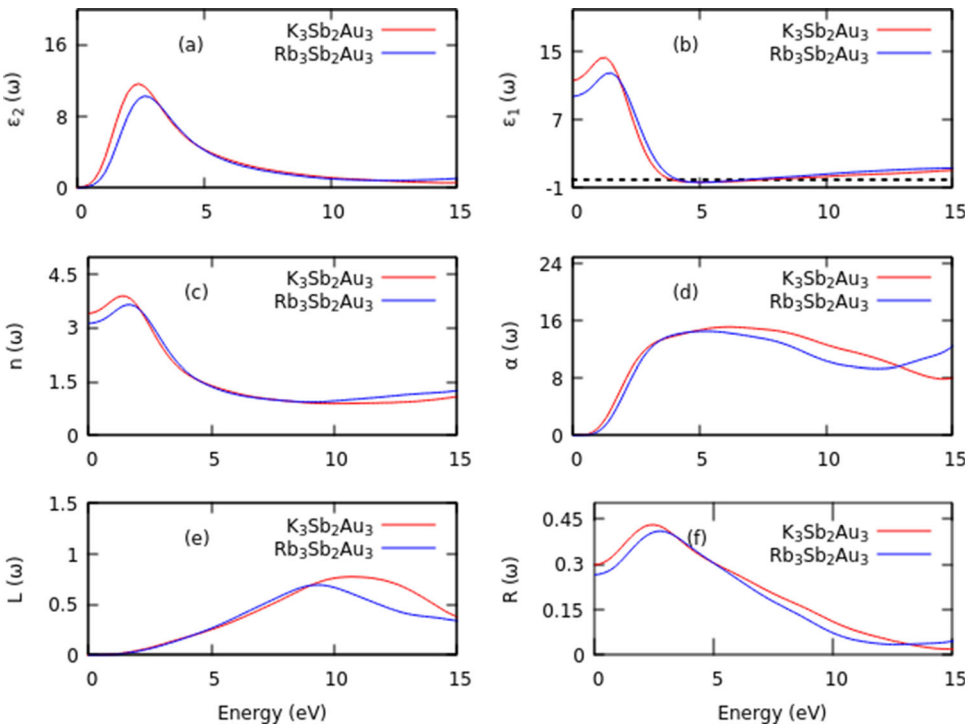

Fig. 5 Computed optical properties of $K_3Sb_2Au_3$ and $Rb_3Sb_2Au_3$ ternary compounds showing (**a**) imaginary dielectric functions, (**b**) real dielectric functions, (**c**) refractive indices, (**d**) absorption coefficients, (**e**) energy loss spectra, and (**f**) reflectivity

frequency limit, $\varepsilon_1(\omega)$ curves attain maximum values at 2.1 eV and 2.6 eV for $K_3Sb_2Au_3$ and $Rb_3Sb_2Au_3$, respectively. At 4–6 eV energy regions, the $\varepsilon_1(\omega)$ curves go below zero. This is the region where the incident photon radiation is said to be fully attenuated [48] and the materials depict a metallic behavior [49]. The number of photons absorbed by a particular medium is measured by the absorption coefficient [17]. Both $K_3Sb_2Au_3$ and $Rb_3Sb_2Au_3$ materials show strong absorption in the energy regions 2.8 eV to 9 eV. These regions cover the UV–Vis part of the electromagnetic spectrum thus the materials under study can be used as UV–Vis absorbers. The refractive index plays a key role in the optical and electronic properties of materials [17]. The major refractive index peaks of both $K_3Sb_2Au_3$ and $Rb_3Sb_2Au_3$ materials lie within the visible region; < 3.1 eV. The obtained values of refractive indices are 3.41 and 3.11 for $K_3Sb_2Au_3$ and $Rb_3Sb_2Au_3$, respectively. These values are in agreement with the ones obtained for compounds with similar crystal structures [6, 50, 51]. The surface behavior of materials is characterized by reflectivity [17]. Small bandgap materials yield large reflectivity values as compared to large bandgap materials [17]. The reflectivity of $K_3Sb_2Au_3$ and $Rb_3Sb_2Au_3$ materials is high in the visible region and it decreases at higher energies. An energy loss function L(ω), represents the energy lost by fast electrons getting into a medium [17]. There were no distinct peaks of L(ω) in the lower energy regions. The major peaks appeared in the

regions 9.66–10.09 eV for both $K_3Sb_2Au_3$ and $Rb_3Sb_2Au_3$ materials.

4. Conclusions

In this work, we have investigated the structural, electronic, elastic, and optical properties of $K_3Sb_2Au_3$ and $Rb_3Sb_2Au_3$ ternary compounds by using density-functional theory. The band structure predicted $K_3Sb_2Au_3$ and $Rb_3Sb_2Au_3$ as semiconductor compounds with direct bandgaps of 1.236 eV and 1.353 eV, respectively. The valence bands have been found to be majorly formed by the Au-4*d* state in the region − 6 to − 3.5 eV with a small contribution from the other states whereas the valence band in the energy regions − 3 eV to the Fermi level was mainly formed by Sb-3*p* with a small contribution from the other states. The conduction band was formed mainly by Sb-3*p* states with low contribution from the other states. The calculated elastic properties show that the materials are mechanically stable and exhibit both ductile and near metallic behaviors. High refractive indices of 3.41 and 3.11 for $K_3Sb_2Au_3$ and $Rb_3Sb_2Au_3$ were obtained, respectively. The optical onsets of the imaginary curves are consistent with the values obtained from the band structure. The calculated optical absorption spectra show that both materials absorb strongly within the UV–Vis (2–9 eV) regions. In summary, $K_3Sb_2Au_3$ and $Rb_3Sb_2Au_3$ ternary compounds were found to be thermodynamically and mechanically stable which makes them easy to synthesize experimentally. Furthermore, direct bandgaps lying between 1 and 1.6 eV are optimal for solar cell applications. High refractive indices and absorption coefficients within the UV–Vis regions make the studied compounds good UV–Vis absorbers hence their suitability for photovoltaic applications.

Acknowledgements The authors acknowledge the Partnership for Skills in Applied Sciences, Engineering and Technology (PASET)—Regional Scholarship Innovation Fund (RSIF) for the Funding opportunity; ISP through the KEN02 grant is thanked for seed funding of computing resources, and gratefully thanked is the Centre for High-Performance Computing, CHPC, Cape Town, RSA, for computing resources.

Declarations

Conflict of interest The authors declare that there were no competing interest.

References

[1] Y Zhong, H Mei, D He and X Du *J. Phys. Chem. Solids* **134** 157 (2019)
[2] K Khan, A Gaur, A Soni, U Ahuja, and J Sahariya *Proc. B-HTC 2020 - 1st IEEE Bangalore Humanit. Technol. Conf.* p 1 (2020)
[3] H Singh and M Singh *AIP Conf. Proc.* **1349** 1069 (2011)
[4] A Es-Smairi, N Fazouan and H Joshi *J. Phys. Chem. Solids* **160** 110305 (2022)
[5] A Gani, O Cheref and M Ghezali *Chin. J. Phys.* **64** 174 (2020)
[6] M Irfan and S Azam *Int. J. Energy Res.* **45** 2980 (2021)
[7] R Li, X Li, L Xi, J Yang and D J Singh *ACS Appl. Mater. Interfaces* **11** 24859 (2019)
[8] M W Iqbal, M Asghar and N A Noor *Phys. Scr.* **96** 125706 (2021)
[9] N Si Ziani, H Bouhani-Benziane, M Baira, A Belfedal, and M Sahnoun *Lecture Notes in Networks and Systems* (Springer International Publishing) **62** 552 (2019)
[10] Q Fan, J Yang and Q Fan *R. Soc. Open Sci.* **4** 170750 (2017)
[11] M Z Rahaman and M A Islam *J. Supercond. Nov. Magn.* **34** 1133 (2021)
[12] S Fahad, G Murtaza and T Ouahrani *J. Alloys Compd.* **646** 211 (2015)
[13] Sibghat-Ullah, G Murtaza, R Khenata, and A H Reshak *Mater. Sci. Semicond. Process*. **26** 79 (2014)
[14] A Sajid *J. Optoelectron. Adv. Mater.* **16** 76 (2014)
[15] G Murtaza *J. Optoelectron. Adv. Mater.* **16** 110 (2014)
[16] P Ranjan, P Kumar, P K Surolia and T Chakraborty *Thin Solid Films* **2** 138469 (2020)
[17] M S Yaseen, J Sun, H Fang, G Murtaza and D S Sholl *Solid State Sci.* **111** 106508 (2021)
[18] N Megag, M Ibrir, M Hadjab and S Berri *Comput. Condens. Matter* **28** e00577 (2021)
[19] P Ranjan and T Chakraborty *Mater. Sci. Semicond. Process.* **127** 105745 (2021)
[20] M H Ali, M H Islam, M Rafid, R Ahmed, M R R Jeetu, R Roy and U Chakma *Eurasian Chem. Commun.* **3** 327 (2021)
[21] M Mirzaei and A H Rasouli *Main Gr. Chem.* **20** 565 (2021)
[22] S F Abdulhussein and S M Abdalhadi *Eurasian Chem. Commun.* **4** 598 (2022)
[23] D M Chapin, C S Fuller and G L Pearson *J. Appl. Phys.* **25** 676 (1954)
[24] J Y Kim, J W Lee, H S Jung, H Shin and N G Park *Chem. Rev.* **120** 7867 (2020)
[25] M J Y Tayebjee, D R McCamey and T W Schmidt *J. Phys. Chem. Lett.* **6** 2367 (2015)
[26] B Ehrler, E Alarcón-Lladó, S W Tabernig, T Veeken, E C Garnett and A Polman *ACS Energy Lett.* **5** 3029 (2020)
[27] A K Singh, J H Montoya, J M Gregoire and K A Persson *Nat. Commun.* **10** 1–19 (2019)
[28] J Mueller and U Zachwieja *Z. Anorg. Allg Chem.* **622** 635 (1996)
[29] F Karsch, A Patkós and P Petreczky *Phys. Lett. Sect. B Nucl. Elem. Part. High-Energy Phys.* **401** 69 (1997)
[30] G Kresse and J Hafner *Phys. Rev. B* **47** 558 (1993)
[31] G Kresse and J Furthmüller *Comput. Mater. Sci.* **6** 15 (1996)
[32] J P Perdew and K Burke *Phys. Rev. Lett.* **77** 3865 (1996)
[33] G Prandini, A Marrazzo, I E Castelli and N Mounet *npj Comput. Mater.* **4** 1 (2018)
[34] T Katsura and Y Tange *Minerals* **9** 1 (2019)
[35] P Ranjan, P Kumar, T Chakraborty and M Sharma *Mater. Chem. Phys.* **241** 122346 (2020)
[36] F Mouhat and F X Coudert *Phys. Rev. B Condens. Matter Mater. Phys.* **90** 224104 (2014)
[37] S Tariq, A Ahmed, S Saad and S Tariq *AIP Adv.* **5** 1 (2015)
[38] V Kumar and B P Singh *Indian J. Phys.* **92** 29 (2018)
[39] S O Karta and T Cagın *J. Alloys Compd.* **508** 177 (2020)
[40] A A Benmakhlouf, A Benmakhlouf and O Allaoui *Chin. J. Phys.* **57** 179 (2019)
[41] N Bioud, X W Sun and N Bouarissa *J. Phys. Sci.* **73** 767 (2018)
[42] H Rekab-Djabri and M Drief *Can. J. Phys.* **98** 834 (2020)
[43] R Bhattacharjee and S Chattopadhyaya *Mater. Chem. Phys.* **199** 295 (2017)

[44] F Giustino, M L Cohen and S G Louie *Phys. Rev. B Condens. Matter. Phys.* **81** 115105 (2010)
[45] A Srivastava, P Sarkar, S K Tripathy and T R Lenka *Sol. Energy* **209** 206 (2020)
[46] G Nazir, S Tariq and A Afaq *Acta Phys. Pol. A* **133** 105 (2018)
[47] F Okbi, S Lakel, S Benramache and K Almi *Semiconductors* **54** 58 (2020)
[48] G Murtaza and I Ahmad *Phys. B Condens. Matter* **406** 3222 (2011)
[49] G Murtaza, B Iftikhar Ahmad, A Amin, M Afaq, J Maqbool, I Maqssod and M Z Khan *Opt. Mater. (Amst)* **33** 553 (2011). https://doi.org/10.1016/j.optmat.2010.10.052
[50] M Mbilo and G S Manyali *Comput. Condens. Matter* **32** e00726 (2022)
[51] R J Musembi and M Mbilo *Materialia* **26** 101587 (2022)